

Improvement of Real-Time Vibration Field Prediction of Structures Through Sensor Signal Noise Reduction

Min Jung Sim*, Byung-Kyoo Jung**, Man-Su Park*** and Weui-Bong Jeong****

Keywords : modal expansion method, modal participation factor, Kalman filter, vibration field visualization

ABSTRACT

This study aimed to develop a model to accurately predict the vibration signal of structural systems in real-time. This paper proposed the method to estimate the real-time vibration field of the whole structure using a limited number of acceleration sensor signals. The modal expansion method (MEM) is the technique to estimate the modal participation factors using the modal matrix and some vibration responses of the structure. In previous studies, MEM has usually been utilized for the estimation of vibration response in the frequency domain. However, MEM for the real-time estimation of vibration field, which uses noise-contaminated acceleration signals, has been hardly studied. Therefore, by using the Kalman filter and MEM, this paper proposed the method not only to reduce the noise in acceleration signal of the time domain but also to estimate the displacement, velocity and acceleration vibration field of a whole structure.

INTRODUCTION

Normally, real-time vibration pattern visualization of the vibration field of structures provides important information for the vibration

Paper Received September, 2019. Revised February, 2020. Accepted February, 2020. Author for Correspondence: Weui-Bong Jeong (wbjeong@pusan.ac.kr).

* Ph. D. Candidate, Department of Mechanical Engineering, Pusan National University, Busan 609-735, Republic of Korea

** Ph. D., Agency for Defence Development, Jinhae, 51678, Republic of Korea

*** Chief Research Engineer, LG Electronics, Changwon, 51554, Republic of Korea

**** Professor, Department of Mechanical Engineering, Pusan National University, Busan 609-735, Republic of Korea

reduction design, the reduction of structure-borne noise, real-time health monitoring, damage diagnosis and real-time control of mechanical systems. Thus, many studies have been conducted to predict the vibration field of structures and to monitor vibration responses using the measured sensor signals.

One of the methods for visualizing the vibration pattern of the structure using the measured sensor signals is the modal expansion method (MEM). Modal expansion techniques seek to estimate the displacements and velocities at all degrees of freedom of a Finite Element (FE) model of a system based on limited measured data which may comprise natural mode shapes or operating deflection shapes.

For many studies, modal expansion method has been used for vibration monitoring (Alkhfaji and Garvey 2013, Cho et al. 2015). Chen et al. (2012) proposed an approach for expanding mode shapes with consideration of both the errors in analytical model and noise in measured modal data. Jung et al. (2016, 2017) introduced the block-wise modal expansion method (BMEM) for reproducing the vibration patterns by dividing the frequency range of interest into several frequency blocks to overcome the problem of a limited number of sensors. Jung and Jeong (2015) predicted the vibration fields and radiation noise of washing machines by applying MEM.

However, from extensive literature reviews, since most of the previous studies conducted on the visualization of vibration fields using conventional modal expansion methods were carried out in a frequency domain, real-time vibration estimation using MEM, which uses noise-contaminated acceleration signals, has been more sparsely represented. Sim et al. (2017), exceptionally, predicted the vibration field of structures by implementing the modal expansion method in a time domain. This paper showed that the more the number of sensors than the number of the mode, the less influence of sensor noise on the vibration field prediction. However, it couldn't overcome the limitation that the more the number of sensors, the

more cost and time consuming.

In fact, there are several limitations to monitor the real-time vibration pattern using the measured sensor signals. First one is that measurement error in vibration test. There is no doubt that a certain level of noise contamination is inevitable in the process of acquiring the vibration signals. Second one is the modeling errors in the finite element model.

In this paper, Kalman filter is used to overcome these limitations. Kalman filter is effective for estimating unmeasured physical quantities, and removing the noise included in the sensor signals (Grewal and Andrews 1992, Zarchan and Musoff 2000). Kalman-filtering-based approaches have been widely used for time domain estimation of mechanical system.

For many studies, Kalman filter has been used for vibration monitoring (Shao and Mechefske 2009), damage diagnosis (Liu et al. 2009, Gao and Lu 2006) and mechanical system identification in time domain (Ghorbani and Cha 2018, Roffel and Narasimhan 2014). For example, Palanisamy et al. (2015) investigated a response estimation technique at unmeasured locations based on the Kalman filter to combine multi-sensor data. Azam et al. (2015) employed a dual Kalman filter to estimate the unknown input and states of a linear state-space model by using sparse noisy acceleration measurements, aiming at prediction of fatigue damage identification. Shrivastava and Mohanty (2018) proposed a model-based method to estimate single plane unbalance parameters (amplitude and phase angle) in a rotor using Kalman Filter.

From broad literature reviews, however, previous studies on estimating vibration responses while minimizing the sensor noise using Kalman-filtering-based approaches were limited. The vibration responses were not be reasonably estimated at points where measurement is not performed. The present article presents a method for real-time visualization and monitoring of a vibration field of an entire structure by using noisy acceleration signals that are measured by a limited number of sensors, which is not larger than the number of modes.

REAL-TIME VIBRATION FIELD PREDICTION THEORY

Time-Domain Vibration Field Prediction Theory

The modal expansion method, one of the vibration field prediction theories, is used to visualize the vibration field of a structure when the number of sensors is limited, by using a characteristic mode matrix obtained by numerical analysis.

The vibration response of a structure is a product of the mode matrix and the modal participation factor (MPF) as shown in Eq. (1).

$$\tilde{\mathbf{x}}(t)_{N \times I} = \mathbf{\Phi}_{N \times m} \ddot{\mathbf{a}}(t)_{m \times I} \quad (1)$$

where $\tilde{\mathbf{x}}(t)$ is the acceleration, $\mathbf{\Phi}$ the natural mode matrix, and $\ddot{\mathbf{a}}(t)$ the acceleration MPF vector.

The subscript, N , is the total degree of freedom of the structure, and m is the number of modes. Therefore, the acceleration signal measured at a point in the structure, $\tilde{\mathbf{x}}(t)$, is expressed as a product of the mode matrix reconstructed only with the values corresponding to the vibration signal acquisition point, $\tilde{\mathbf{\Phi}}$, and the MPF, $\ddot{\mathbf{a}}(t)$, as shown in Eq. (2) where the subscript, n , denotes the number of sensors.

$$\tilde{\mathbf{x}}(t)_{n \times I} = \tilde{\mathbf{\Phi}}_{n \times m} \ddot{\mathbf{a}}(t)_{m \times I} \quad (2)$$

The modal expansion method employed the pseudo-inverse matrix of the reconstructed mode matrix, $\tilde{\mathbf{\Phi}}^\dagger$, as shown in Eq. (3). To obtain appropriate results from the estimated MPF vector which is calculated using the pseudo-inverse matrix, the number of sensors used, n , should be greater than the number of modes used, m .

$$\tilde{\tilde{\mathbf{a}}}(t)_{m \times I} = \tilde{\mathbf{\Phi}}^\dagger_{m \times n} \tilde{\mathbf{x}}(t)_{n \times I} \quad (3)$$

$\tilde{\tilde{\mathbf{a}}}(t)$ is the acceleration MPF vector estimated by the modal expansion method. The estimated acceleration MPF, $\tilde{\tilde{\mathbf{a}}}(t)$, reflects the incoming noise signals from the sensors. Therefore, the vibration field of a structure estimated by using the estimated acceleration MPF, $\tilde{\tilde{\mathbf{a}}}(t)$, is different from the actual vibration field due to the influence of the noise. The present article proposes a real-time vibration field estimation method for reducing the sensor noise.

Modeling of a System State Space

A state space model was designed to analyze the system in the time domain. The state space expressing the system is expressed in Eqs. (4)-(5).

$$\mathbf{X}_{k+I} = \mathbf{A}\mathbf{X}_k + \mathbf{B}\mathbf{F}_k \quad (4)$$

$$\mathbf{Y}_k = \mathbf{C}\mathbf{X}_k + \mathbf{D}\mathbf{F}_k \quad (5)$$

where \mathbf{X} is the state variable vector, \mathbf{Y} is the measurement vector, and \mathbf{F} is the force vector in the physical coordinates. The subscript, k , refers to time.

Generally, Eq. (4) is derived from the equation of motion of the system. Eq. (5) shows the relations between the measurements and the state variables, specifying how the state variable is reflected in the measurements. The equation of motion in the mode

coordinates used to express Eq. (4) for the state space model is shown in Eq. (6). Here, the subscript, r , means that the value corresponds to the r -th mode among the modes used for the modal expansion method. Hence, \ddot{a}_r is the acceleration MPF of the r -th mode, \dot{a}_r is the velocity MPF, a_r is the displacement MPF, q_r is the force in the r -th modal coordinates, ζ_r is the damping ratio, and ω_r is the natural frequency.

$$\ddot{a}_r + 2\zeta_r\omega_r\dot{a}_r + \omega_r^2a_r = q_r \quad (6)$$

The state variable, \mathbf{X} , is defined as Eq. (7). In Eq. (7), \mathbf{a} and $\dot{\mathbf{a}}$ respectively refer to the displacement MPF vector and the velocity MPF vector, which are expressed as Eqs. (8)-(9).

$$\mathbf{X}_{2m \times 1} = \begin{Bmatrix} \mathbf{a} \\ \dot{\mathbf{a}} \end{Bmatrix} \quad (7)$$

$$\mathbf{a}_{m \times 1} = \{a_1, a_2, a_3, \dots, a_r, \dots, a_m\}^T \quad (8)$$

$$\dot{\mathbf{a}}_{m \times 1} = \{\dot{a}_1, \dot{a}_2, \dot{a}_3, \dots, \dot{a}_r, \dots, \dot{a}_m\}^T \quad (9)$$

The force in the modal coordinates, \mathbf{q} , expressed as in Eq. (10), is related to the force in the physical coordinates, \mathbf{F} , as shown in Eq. (11).

$$\mathbf{q}_{m \times 1} = \{q_1, q_2, q_3, \dots, q_r, \dots, q_m\}^T \quad (10)$$

$$\mathbf{q}_{m \times 1} = \Phi_{m \times N}^T \mathbf{F}_{N \times 1} \quad (11)$$

Now, the matrices \mathbf{A} and \mathbf{B} in Eq. (4) are expressed by Eqs. (12)-(15).

$$\mathbf{A} = \mathbf{I}_{2m \times 2m} + \Delta t \begin{bmatrix} \mathbf{0}_{m \times m} & \mathbf{I}_{m \times m} \\ -\mathbf{\Omega}^2_{m \times m} & -2\mathbf{Z}\mathbf{\Omega}_{m \times m} \end{bmatrix} \quad (12)$$

$$\mathbf{B} = \begin{bmatrix} \mathbf{0}_{m \times N} \\ \Delta t \Phi_{m \times N}^T \end{bmatrix} \quad (13)$$

$$\mathbf{\Omega} = \begin{bmatrix} \omega_1 & & & & & \\ & \omega_2 & & & & \\ & & \ddots & & & \\ & & & \omega_r & & \\ & & & & \ddots & \\ & & & & & \omega_m \end{bmatrix} \quad (14)$$

$$\mathbf{Z} = \begin{bmatrix} \zeta_1 & & & & & \\ & \zeta_2 & & & & \\ & & \ddots & & & \\ & & & \zeta_r & & \\ & & & & \ddots & \\ & & & & & \zeta_m \end{bmatrix} \quad (15)$$

For the modeling of the matrices, \mathbf{C} and \mathbf{D} , the measurement, \mathbf{Y} , is defined in Eq. (16) as the acceleration signal, $\tilde{\mathbf{x}}$, measured at n sensors at some points on the structure.

$$\mathbf{Y} = \tilde{\mathbf{x}}_{n \times 1} \quad (16)$$

The modal expansion method, shown in Eq. (2), is used to express the relation between the measurement, \mathbf{Y} , and the acceleration MPF vector, $\ddot{\mathbf{a}}_{m \times 1}$, as in Eqs. (17)-(18).

$$\ddot{\mathbf{a}}_{m \times 1} = \{\ddot{a}_1, \ddot{a}_2, \ddot{a}_3, \dots, \ddot{a}_r, \dots, \ddot{a}_m\}^T \quad (17)$$

$$\mathbf{Z} = \tilde{\Phi}_{n \times m} \ddot{\mathbf{a}}_{m \times 1} \quad (18)$$

By using Eq. (6), the acceleration MPF vector may be expressed with respect to the modes as shown in Eq. (19).

$$\ddot{\mathbf{a}}_{m \times 1} = [-\mathbf{\Omega}^2 - 2\mathbf{Z}\mathbf{\Omega}]_{m \times 2m} \begin{Bmatrix} \mathbf{a} \\ \dot{\mathbf{a}} \end{Bmatrix}_{2m \times 1} + \mathbf{q}_{m \times 1} \quad (19)$$

Using the Eq. (11) to convert the force vector in the modal coordinates to the one in the physical coordinates, the matrices, \mathbf{C} and \mathbf{D} , may be expressed as Eqs. (20)-(21).

$$\mathbf{C} = \tilde{\Phi}_{n \times m} [-\mathbf{\Omega}^2 - 2\mathbf{Z}\mathbf{\Omega}]_{m \times 2m} \quad (20)$$

$$\mathbf{D} = \tilde{\Phi}_{n \times m} \Phi_{m \times N}^T \quad (21)$$

Noise Reduction Filter

Using A Kalman filter, it is possible to estimates the state variables in real-time under a minimized noise influence. Here, the measured noise and the noise inflowing to the system are assumed to be white Gaussian noise.

Adding the white Gaussian noise to the Eqs. (4)-(5), the state space of a system without considering the noise, the state space is expressed as the Eqs. (22)-(23) where \mathbf{w}_k is the noise vector inflowing to the system affecting the state variable, and \mathbf{v}_k is the measured noise vector.

$$\mathbf{X}_{k+1} = \mathbf{A}\mathbf{X}_k + \mathbf{B}\mathbf{F}_k + \mathbf{w}_k \quad (22)$$

$$\mathbf{Y}_k = \mathbf{C}\mathbf{X}_k + \mathbf{D}\mathbf{F}_k + \mathbf{v}_k \quad (23)$$

From these noise vector, the covariant matrices can be defined. \mathbf{Q} is the covariance matrix of \mathbf{w}_k , and \mathbf{R} is the covariance matrix of \mathbf{v}_k .

Fig. 1 shows the algorithm of the Kalman filter. The Kalman filter algorithm consists of a prediction process and an estimation process. The prediction process is based on Eq. (22), which shows how the

system moves over time. The estimation process is based on Eq. (23). The estimation process is a process of updating the predicted values in the previous step using the measured values, which shows the relationship between measurements and state variables.

In Fig. 1, \mathbf{P}_k denotes the error covariance, and \mathbf{K}_k denotes the Kalman gain. The superscript, \wedge , denotes that the value is an estimated, and the superscript, $\bar{}$, means that the value is a predicted. The prediction process predicts the values of the state variable, \mathbf{X} , and the error covariance, \mathbf{P} , based on the system model. In other words, in the prediction process, the estimated state variables of the previous step, $\hat{\mathbf{X}}_{k-1}$, and the error covariance of the previous step, \mathbf{P}_{k-1} , are used to calculate the predicted state variables, $\hat{\mathbf{X}}_k^-$, and the predicted covariance values, \mathbf{P}_k^- .

The estimation process is the process for compensating the difference between the sensor measurements and the predicted values. In other words, the predicted state variables, $\hat{\mathbf{X}}_k^-$, and the predicted covariance, \mathbf{P}_k^- , obtained in the prediction process are used to calculate the Kalman gain, \mathbf{K}_k , the estimated state variables, $\hat{\mathbf{X}}_k$, and the error covariance, \mathbf{P}_k . These two processes are repeated in each of the steps to estimate the optimal state variables in real-time.

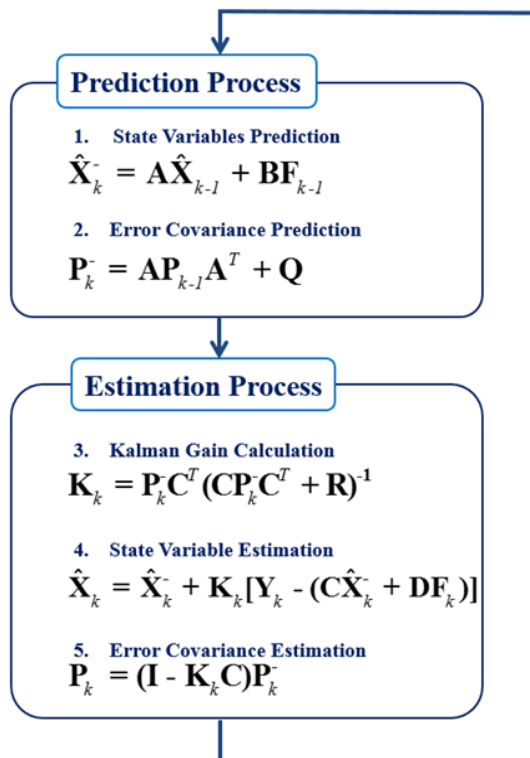


Fig. 1. Kalman filter algorithm

Visualization of Vibration Field Using State Variables

Estimating the state variables using the presented Kalman filter enables estimation of the displacement, velocity, and acceleration vibration of an entire structure.

The state variables, \mathbf{X} , consist of the displacement MPF vectors and the velocity MPF vectors for the modes used in the modal expansion method. Hence, the displacement vector of the entire structure, \mathbf{x} , and the velocity vector of the entire structure, $\dot{\mathbf{x}}$, may be estimated by using Eqs. (24)-(25).

$$\mathbf{x}_{N \times 1} = \Phi_{N \times m} \mathbf{a}_{m \times 1} \tag{24}$$

$$\dot{\mathbf{x}}_{N \times 1} = \Phi_{N \times m} \dot{\mathbf{a}}_{m \times 1} \tag{25}$$

Also, the acceleration MPF may be obtained from the state variables, \mathbf{X} , by using Eq. (18). Therefore, the acceleration vibration response of the entire structure, $\ddot{\mathbf{x}}$, may be estimated by using Eq. (26).

$$\ddot{\mathbf{x}}_{N \times 1} = \Phi_{N \times m} \ddot{\mathbf{a}}_{m \times 1} \tag{26}$$

ANALYSIS AND RESULT

Analytical Model

The analytical model used in the present study is a planar structure in which four vertices are bound at six degrees of freedom. The shape of the finite element model for the structure (510 nodal points and 464 elements) is shown in Fig. 2. The positions of the uniformly arranged sensors, the positions and directions of excitation and the arbitrarily selected position for comparing the estimated results are also shown in Fig. 2. The 5 mm-thick planar structure was made of steel. Table 1 shows the physical properties of the structure.

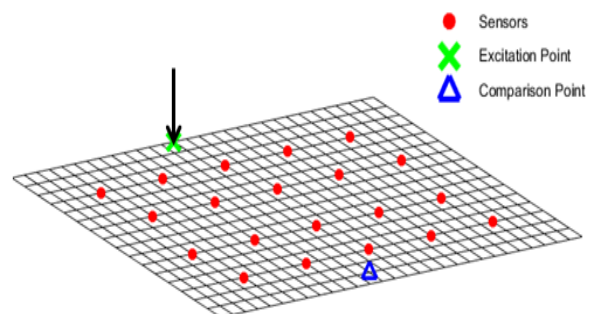


Fig. 2. Geometry of plate, positions of sensors, excitation point and comparison point.

The vibration responses of the entire structure

without the noise, which are used as the reference signals in this study, were obtained by performing the transient response analysis using MCS. Nastran.

Table 1. Properties of steel

Density	7850 kg m ⁻³
Young's modulus	210 GPa
Poisson's ratio	0.3

In the present study, a total of 20 modes used for the modal expansion method, from the 1st mode to the 20th mode, were obtained by the eigenvalue analysis performed MCS. Nastran. The number of sensors used was 20, and the sensors were arranged uniformly as shown in Fig. 2. The signals measured by the sensors were assumed to be the signals obtained by adding white Gaussian noise to the acceleration vibration responses resulting from the transient vibration analysis using MCS. Nastran. To evaluate the robustness of the proposed method, high levels of noise in the measured response data are considered.

Prediction of a Vibration Field Under Periodic Excitation

Prediction of a Vibration Field Under Sine Wave Excitation

The steady-state vibration field of the structure was predicted under excitation with a sine wave of 10 Hz, as shown in Fig. 3. The signals measured at the sensors were assumed to be the signals obtained by adding white Gaussian noise with a standard deviation of 0.05 ms⁻² to the acceleration vibration responses obtained from the transient response analysis. The signal-to-noise ratio (SNR) of the acceleration signals measured by the sensors was 11 [dB].

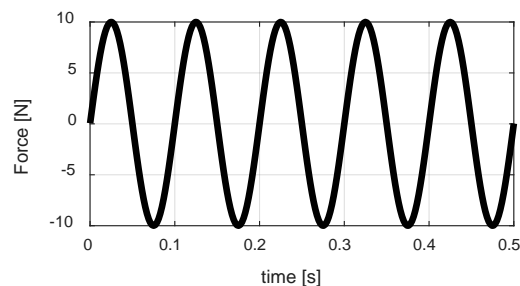
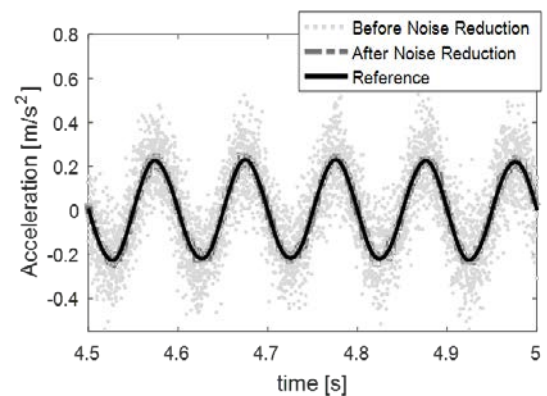


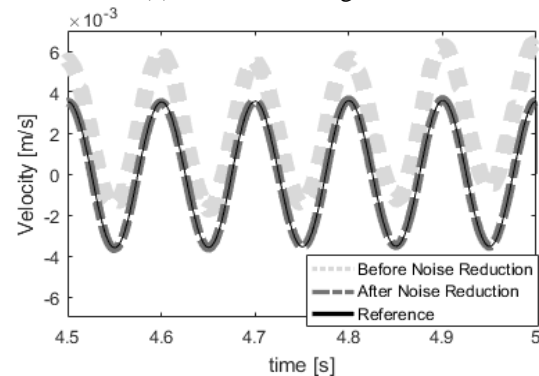
Fig. 3. Sinusoidal wave force

To verify the steady-state vibration signal estimation performance of the Kalman filter for the acceleration, velocity, and displacement, the vibration response plots at the unmeasured point, which is arbitrarily selected, marked as Δ in Fig. 2, are shown in Fig. 4.

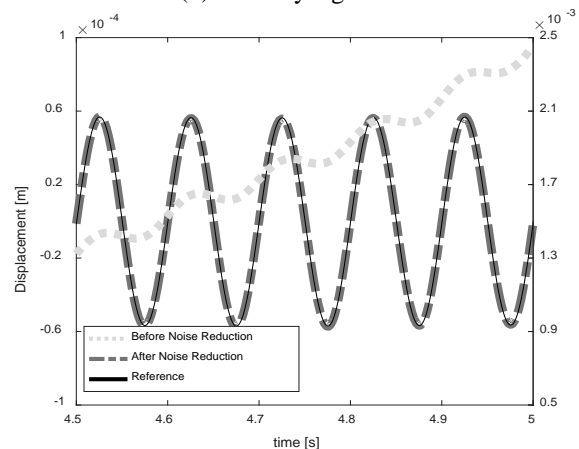
The solid line in Fig. 4 represents the reference vibration response signals, while the dotted line represents the 'vibration response signals affected by the noise.' The dash-single dotted line represents the 'vibration response signals estimated by minimizing the influence of the noise'. In the plot shown in Fig. 4(c), the y-axis range of the signals represented by the dotted line is on the right-side range of the y-axis, in contrast to the two other signals. The 'velocity signals and displacement signals affected by the noise' were obtained through numerical integration of the acceleration signals mixed with the noise.



(a) Acceleration signals



(b) Velocity signals



(c) Displacement signals

Fig. 4. Real-time vibration estimation of the structure subjected to the sinusoidal wave force

The plot shown in Fig. 4(a) indicates that the noise measured at the acceleration sensors was reduced in the signals estimated by reducing the influence of the noise. The plots shown in Figs. 4(b)-(c) show that the error caused by the noise was accumulated and diverged over time in the 'velocity signals and displacement signals affected by the noise.' In contrast, 'velocity signals and displacement signals estimated by reducing the influence of the noise' well estimated the reference response signals.

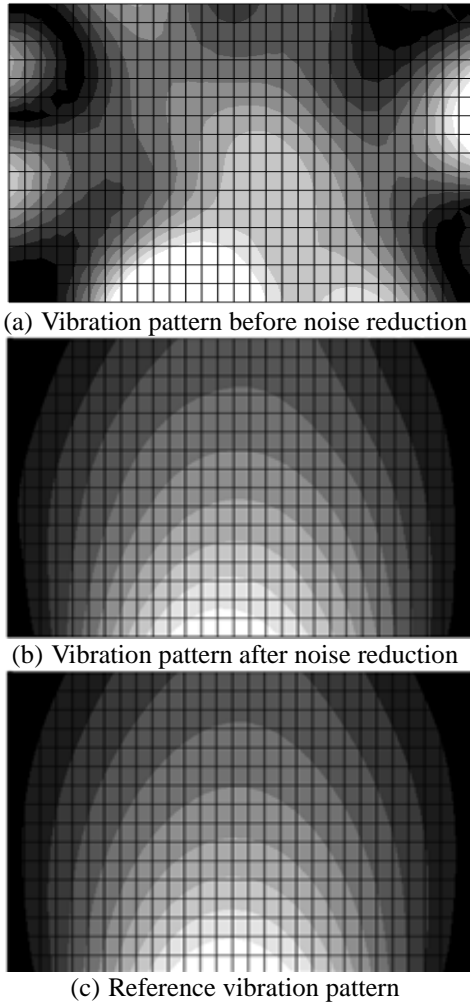


Fig. 5. Vibration patterns of the structure at 4.912 s subjected to the sinusoidal wave force

Fig. 5 shows the plot for the acceleration vibration field at an arbitrary time point of 4.912 s in a steady state, when the excitation was performed by using a sine wave, to investigate the vibration field prediction performance of the Kalman filter. Fig. 5(a) shows the predicted acceleration vibration field without filtering the noise-contaminated signal. Fig. 5(b) shows the estimated acceleration vibration field representing the signals with reduced measurement noise influence, and Fig. 5(c) shows the reference vibration field. The result shown in Fig. 5 indicates

that the reference acceleration vibration field was estimated relatively accurately in the estimation of the vibration field using the Kalman filter, because the influence of the noise was removed from the sensor signals.

To investigate the ability of the Kalman filter to estimate steady-state acceleration, velocity, and displacement, a normalized error rate was defined as shown in Eq. (27).

$$e_s = \frac{\frac{1}{N} \sum_{j=1}^N \left[\int_0^{T^F} (v_j(t) - v_j^{\text{ref}}(t))^2 dt \right]}{\frac{1}{N} \sum_{j=1}^N \left[\int_0^{T^F} (v_j^{\text{ref}}(t))^2 dt \right]} \quad (\%) \quad (27)$$

where N is the number of nodes in the entire structure, T^F is the period of the excitation force, and j is the numbering of the nodes. $v_j^{\text{ref}}(t)$ denotes the reference vibration signals, and $v_j(t)$ denotes the vibration signal of the estimated acceleration, velocity, and displacement.

Table 2. Normalized errors of the vibration signal subjected to the sinusoidal wave force

	Normalized Error, e_s (%)	
	Conventional	Proposed
Acceleration	58.6	1.25
Velocity	diverged	0.0226
Displacement	diverged	0.00950

Table 2 shows the normalized error rate of the acceleration, velocity, and displacement subjected to the sine wave excitation. The estimation error of the acceleration responses by the conventional method without using Kalman filter was 58.6%, but the error rate was significantly decreased to 1.28% in the vibration response signals predicted by using the Kalman filter. While the velocity and displacement diverged in the conventional prediction method, they converged in the prediction method proposed in this article within a certain error rate.

Prediction of a Vibration Field Under Triangular Wave Excitation

The steady-state vibration field was predicted under excitation with a triangular wave of 10 Hz, as shown in Fig. 6. The signals measured at the sensors were assumed to be the signals obtained by adding white Gaussian noise with a standard deviation of 0.05 ms^{-2} to the acceleration vibration responses obtained from the transient response analysis. The signal-to-noise ratio (SNR) of the acceleration signals measured by the sensors was 11 [dB].

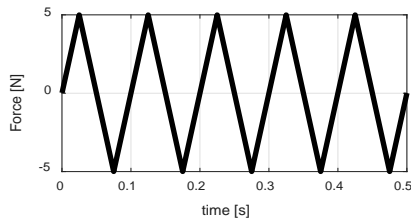


Fig. 6. Triangular wave force

To verify the steady-state vibration signal estimation performance of the Kalman filter, the vibration response plots at arbitrary selected point, marked as Δ , are shown in Fig. 7, which are response plot under triangular wave excitation.

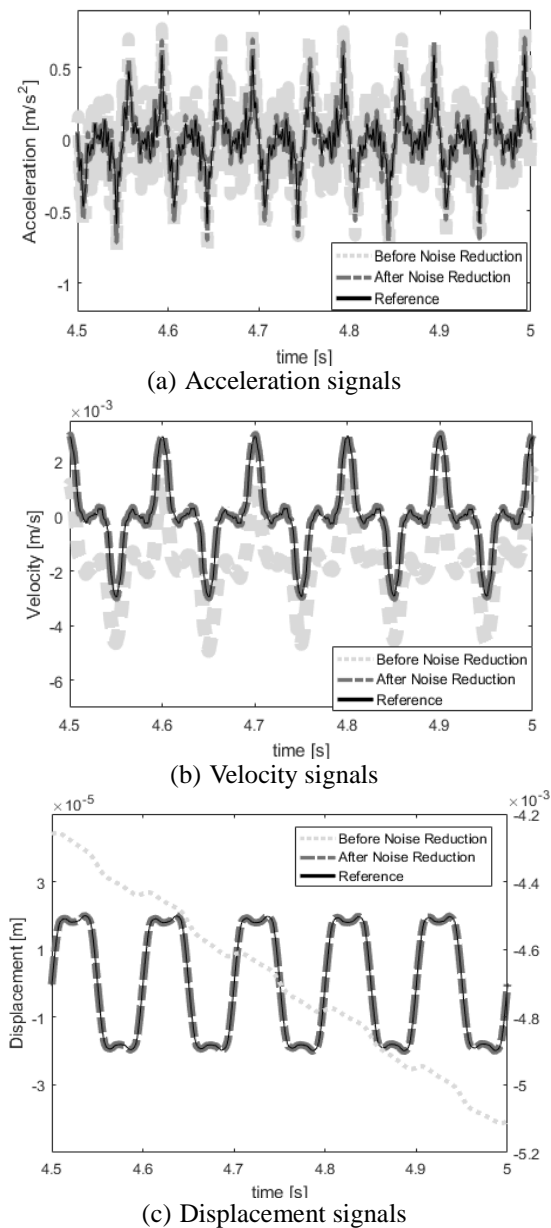


Fig. 7. Real-time vibration estimation of the structure subjected to triangular wave force

The meaning of the individual types of lines in Fig. 7 are the same as in Fig. 4. Similarly, in the plot shown in Fig. 7(c), the y-axis range of the signals represented by the dotted line is on the right-side range of the y-axis, in contrast to the two other signals.

The result shown in Fig. 7 is similar to the result shown in Fig. 5 representing the result under sine wave excitation. The acceleration plot shown in Fig. 7(a) indicates that the measurement noise was reduced in the acceleration signals estimated by Kalman filter suggested in this paper. The plots in Figs. 7(b)-(c) indicate that the velocity and displacement signals, obtained by numerical integration, diverged over time. On the other hand, the velocity and displacement signals estimated by using the filter well estimated the reference vibration response.

Fig. 8 shows the plot for the acceleration vibration field at the time point of 4.912 s, which is in a steady state under a triangular wave excitation.

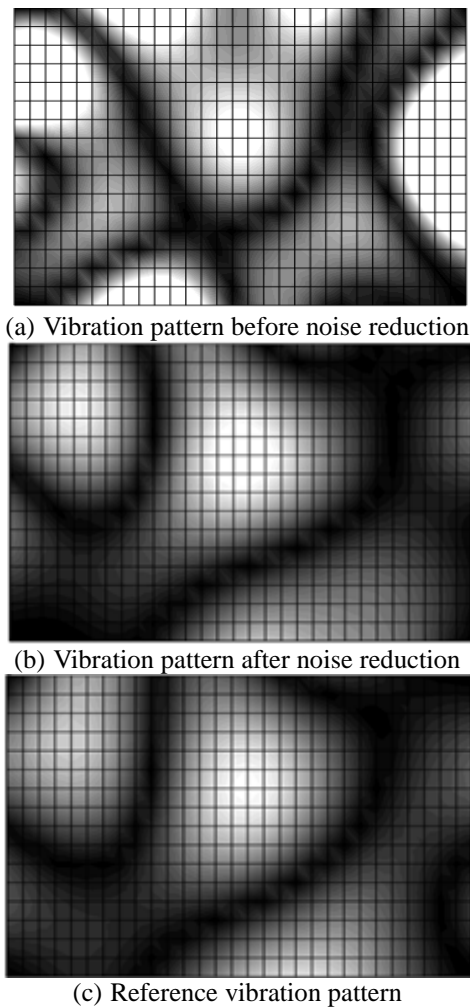


Fig. 8. Vibration patterns of the structure at 4.901 s subjected to the triangular wave force

The meanings of the plots in Figs. 8(a)-(c) are the same as the plots in Fig. 6. The result shown in Fig. 8 indicates that the reference acceleration vibration field was estimated relatively accurately in the estimation of the vibration field using the Kalman filter, reducing the influence of measurement noise.

Similar to the case of the sine wave excitation, the normalized error in the acceleration, velocity, and displacement estimation calculated by Eq. (26) is shown in Table 3.

The error rate in the acceleration was reduced from 132% in the case where no filter was applied to 5.44% in the case where the Kalman filter was applied. While the velocity and displacement diverged in the conventional prediction method, they converged in the prediction method proposed in this study within a certain error rate.

Table 3. Normalized errors of the vibration signal subjected to the triangular wave force

	Normalized Error, e_s (%)	
	Conventional	Proposed
Acceleration	132	5.44
Velocity	diverged	0.0745
Displacement	diverged	0.00902

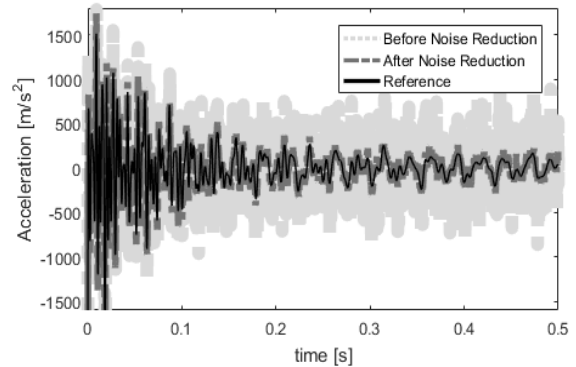
Prediction of a Vibration Field Under Nonperiodic Excitation

A transient-state vibration field was predicted when the structure was excited with a unit impact. The acceleration signals measured at the sensors were assumed to be the signals obtained by adding white Gaussian noise with a standard deviation of 100 ms^{-2} to the acceleration vibration responses obtained from the transient response analysis. Since the power of the vibration signals is continuously reduced over time in a unit impact response, for convenience's sake the magnitude of the noise signal was selected to be the value that made the SNR 11 dB with respect to the signal received for 0.1 second from the moment when the unit impact applied.

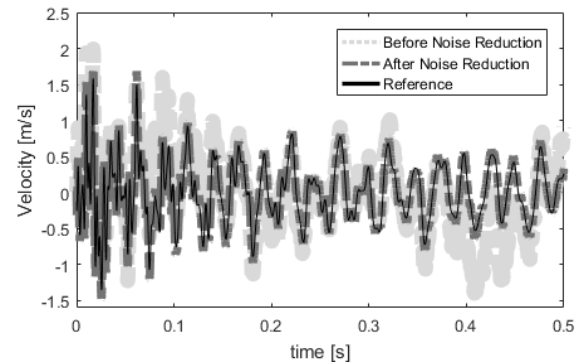
To verify the transient-state vibration signal estimation performance for the acceleration, velocity, and displacement, the vibration response plots at arbitrary selected point, marked as Δ , are shown in Fig. 9, which is a transient-state vibration response graph. The meanings of the individual types of lines in Figs. 9(a)-(c) are the same as in Fig. 4. Similarly, in the plot shown in Fig. 7(c), the y-axis range of the signals represented by the dotted line is on the right-side range of the y-axis, in contrast to the two other signals.

The result shown in Fig. 9 is similar to the results obtained under periodic excitation. The acceleration plot shown in Fig. 9(a) indicates that the noise measured at the acceleration sensors was reduced in the acceleration responses estimation. The

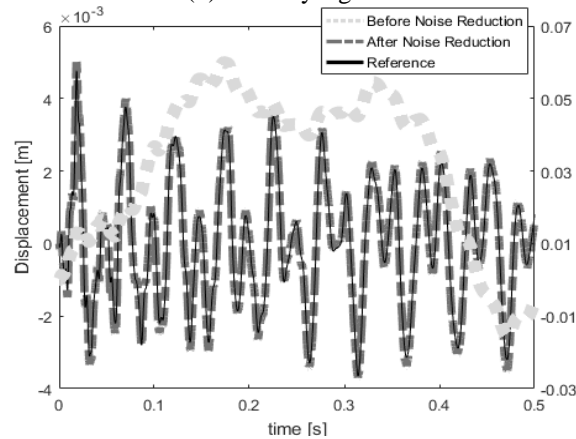
plots in Figs. 7(b)-(c) indicate that the velocity and displacement signals, obtained by numerical integration, diverged over time. However, the 'velocity and displacement signals estimated by minimizing the influence of the noise' well estimated the reference vibration responses.



(a) Acceleration signals



(b) Velocity signals



(c) Displacement signals

Fig. 9. Real-time vibration estimation of the structure subjected to the unit impulse

Fig. 10 shows the plot for the acceleration vibration field at an arbitrary time point of 0.100 s, which is in a transient state, when the plate is subjected to the unit impact. The meanings of the plots in Figs 10(a)-(c) are similar with the plots in Fig. 5. The result shown in Fig. 10 indicates that the reference acceleration vibration field was estimated

relatively accurately in the estimation of the vibration field using the Kalman filter, because the influence of the measurement noise was removed from the sensor signals.

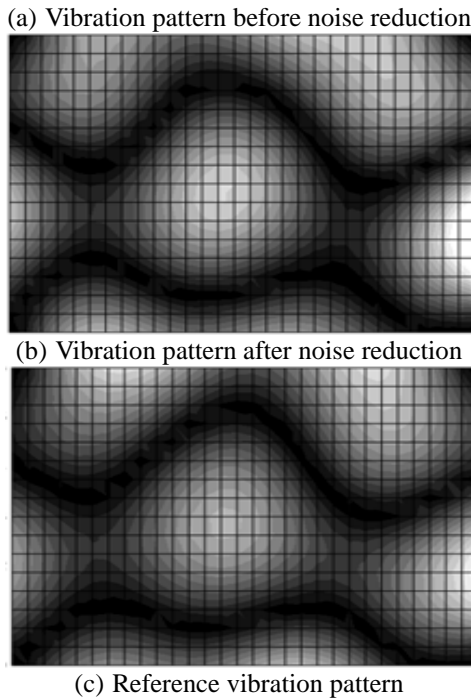


Fig. 10. Vibration patterns of the structure at 0.100 s subjected to the unit impulse

To investigate the ability of the Kalman filter to estimate the transient-state acceleration, velocity, and displacement, the error rate was calculated. To determine the time range for the evaluation of the error rate of the transient-state signal, for convenience's sake the time at which the energy level of the acceleration response signals reaches 95% of the acceleration energy level for the whole time was defined as T^T .

Using the calculated T^T , the vibration field prediction error rate for the transient-state response signals was defined, as shown in Eq. (28).

$$e_T = \frac{\frac{1}{N} \sum_{j=1}^N \left[\int_0^{T^T} (v_j(t) - v_j^{\text{ref}}(t))^2 dt \right]}{\frac{1}{N} \sum_{j=1}^N \left[\int_0^{T^T} (v_j^{\text{ref}}(t))^2 dt \right]} \quad (\%) \quad (28)$$

Table 4 compares the estimation error rate of the transient-state response signals for the conventional method and the method proposed in the present paper.

Table 4 shows that the error rate was 81.5% in the case where the Kalman filter was not applied, but it was decreased to 4.43% in the case where the Kalman filter was applied. While the velocity and displacement diverged in the conventional prediction method, they converged in the prediction method proposed in this article within a certain error rate. The estimated velocity and displacement diverged as the error calculated by the numerical integration was accumulated, but they stably converged because the error was small in the method proposed in this paper.

Table 4. Normalized errors of the vibration signal subjected to the unit impulse

	Normalized Error, e_T (%)	
	Conventional	Proposed
Acceleration	81.5	4.43
Velocity	diverged	2.89
Displacement	diverged	0.64

CONCLUSIONS

This paper proposes a highly accurate real-time method for estimating a vibration field from noisy acceleration sensor signals. The displacement, velocity and acceleration field were obtained from the state variables of the Kalman filter, to which the modal expansion method was applied.

In order to validate the ability of the presented method, 'the vibration response at unmeasured points' was compared under various excitation conditions. Under both periodic excitation and nonperiodic excitation, the acceleration, velocity, and displacement vibration fields were estimated.

Under various excitation conditions, the real-time vibration fields predicted by the method without using Kalman filter diverged, because the error was continuously accumulated in the process of performing numerical integration of the measured signals. In contrast, when using the presented method that can reflect the system characteristics, the predicted vibration field did not diverge and could be predicted.

In the case where the vibration field is to be estimated from the noisy acceleration signals obtained from a limited number of sensors, this presented noise-reducing filter may be useful to estimate the real time vibration field of an entire structure, minimizing the influence of the noise.

Although the presented study was conducted with a planar structure, the method proposed in this

article may be applied to structures having a more complicated shape, to estimate and monitor the vibration response of the structures.

REFERENCES

- Alkhfaji, S.S., Garvey, S.D., “Frequency dependent operations for 2nd order systems—modal expansion and modal correlation”, *Journal of Sound and Vibration*, Vol. 332, No. 4, pp.1033-1046 (2013).
- Azam, S.E., Chatzi, E., Papadimitriou, C., “A dual Kalman filter approach for state estimation via output-only acceleration measurements”, *Mechanical Systems and Signal Processing*, Vol. 60, pp.866-886 (2015).
- Chen, H.P., Tee, K.F., Ni, Y.Q., “Mode shape expansion with consideration of analytical modeling errors and modal measurement uncertainty”, *Smart Structures and Systems*, Vol. 10, No. 4, pp.485-499 (2012).
- Gao, F., Lu, Y., “A Kalman-filter based time-domain analysis for structural damage diagnosis with noisy signals”, *Journal of Sound and Vibration*, Vol. 297, No. 4, pp.916-930 (2006).
- Ghorbani E., Cha, Y.-J., “An iterated cubature unscented Kalman filter for large-DoF systems identification with noisy data”, *Journal of Sound and Vibration*, Vol. 420, pp.21-34 (2018).
- Grewal, M.S., Andrews, A.P., *Kalman Filtering: Theory and Practice Using MATLAB*, John Wiley and Sons, New York, N.Y. (1992).
- Jung, B.K., Cho J., Jeong W.B., “Sensor placement optimization for structural modal identification of flexible structures using genetic algorithm”, *Journal of Mechanical Science and Technology*, Vol. 29, No. 7, pp.2775-2783 (2015).
- Jung, B.K., Cho J., Jeong W.B., “Reproduction of vibration patterns of elastic structures by block-wise modal expansion method (BMEM)”, *Smart Structures and Systems*, Vol. 18, No. 4, pp.819-837 (2016).
- Jung, B.K., Jeong W.B., “Mode selection of modal expansion method estimating vibration field of washing machine”, *Journal of Sound and Vibration*, Vol. 340, pp.343-353 (2015).
- Jung, B.K., Jeong W.B., Cho J., “Improved block-wise MET for estimating vibration fields from the sensor”, *STRUCTURAL ENGINEERING AND MECHANICS*, Vol. 64, No. 3, pp.279-285 (2017).
- Liu, X., Escamilla-Ambrosio, P.J., Lieven, N., “Extended Kalman filtering for the detection of damage in linear mechanical structures”, *Journal of Sound and Vibration*, Vol. 325, No. 4, pp.1023-1046 (2009).
- Palanisamy, R.P., Cho, S., Kim, H., Sim, S., “Experimental validation of Kalman filter-based strain estimation in structures subjected to non-zero mean input”, *Smart Structures and Systems*, Vol. 15, No. 2, pp.489-503 (2015).
- Roffel, A., Narasimhan, S., “Extended Kalman filter for modal identification of structures equipped with a pendulum tuned mass damper”, *Journal of Sound and Vibration*, Vol. 333, No. 23, pp.6038-6056 (2014).
- Shao, Y., Mechefske, C.K., “Gearbox vibration monitoring using extended Kalman filters and hypothesis tests”, *Journal of Sound and Vibration*, Vol. 325, No. 3, pp.629-648(2009).
- Shrivastava, A., Mohanty, A., “Estimation of single plane unbalance parameters of a rotor-bearing system using Kalman filtering based force estimation technique”, *Journal of Sound and Vibration*, Vol. 418, pp.184-199 (2018).
- Sim, M.J., Jung, B.K., Oh, H.E., Jeong W.B., “Vibration field estimation of the structure in time domain using noise-contaminated sensor signals”, *Transactions of Korean Society for Noise and Vibration Engineering*, Vol. 27, No. 6, pp.705-712 (2017).
- Zarchan, P., Musoff, H., *Fundamentals of Kalman Filtering: A Practical Approach*, American Institute of Aeronautics and Astronautics, Reston, Virginia, USA (2000)